NONLINEAR DYNAMICS ON PARAMETRIC ROLLING OF SHIPS IN HEAD SEAS

Marcelo A. S. Neves, LabOceano, COPPE/UFRJ, masn@peno.coppe.ufrj.br
Jerver E. M. Vivanco, COPPE/UFRJ, jervermv@peno.coppe.ufrj.br
Claudio A. Rodríguez, LabOceano, COPPE/UFRJ, claudiorc@peno.coppe.ufrj.br

ABSTRACT

The present paper employs nonlinear dynamics tools in order to investigate the dynamical characteristics governing the complex coupling of the heave, roll and pitch modes in head seas at some regions of the numerical stability map of a fishing vessel. Bifurcation diagrams and Poincaré mappings are computed and employed to investigate the appearance of multistability and chaos associated with increased values of the selected control parameter, the wave amplitude. The connection between these nonlinear characteristics and the coupled nature of the mathematical model are analyzed. Lyapunov exponents corresponding to the three coupled models are computed.

Keywords: *Parametric resonance, bifurcation, multistability, chaos, lyapunov exponents*

1. INTRODUCTION

It is well known that parametric rolling in head seas may lead to large roll angles and accelerations in few cycles. Even though many studies on the subject simplify the analysis to a single degree of freedom, there is nowadays a wide acceptance of the relevance of the nonlinear coupling of the roll mode with heave and pitch.

In previous studies Neves and Rodríguez (2005, 2006) have introduced a mathematical model in which the heave, roll and pitch motions are nonlinearly coupled to each other. Using this model they investigated the occurrence of head seas parametric rolling on a small fishing vessel. They showed, by means of numerical simulations, comparable to experimental results, the occurrence of strong dependence of the roll responses in head seas conditions on initial conditions, Neves and Rodríguez (2007).

In order to investigate the quantitative and qualitative changes of parametric rolling with respect to the encounter frequency tuning and wave amplitude, Neves and Rodríguez (2007a,b) proposed the computation of analytical and numerical maps representing the boundaries of stability. The numerical maps aggregate information not only on the boundaries of stability, but also on the amplitude of roll response in the whole region of parametric amplification.

The present paper investigates the dynamical characteristics governing the complex coupling of modes at some regions of the numerical stability map. Bifurcation diagrams and Poincaré mappings, Guckenheimer and Holmes (1983), Seydel (1988) are employed in order to investigate the appearance of multistability and chaos associated with increased values of the control parameter wave amplitude. The connection between these nonlinear characteristics and the coupled nature of the model are analyzed. Finally, Lyapunov exponents corresponding to the three coupled models are computed.

2. MATHEMATICAL MODEL

Employing Taylor series expansions up to third order, Neves and Rodríguez (2005, 2006) expressed restoring actions in the heave, roll and pitch modes in a coupled way. Wave actions are taken into consideration not only in the Froude-Krilov plus diffraction first order forcing functions, but also in second and third order terms resulting from volumetric changes of the submerged hull due to vertical motions and wave passage effects. The model corresponds to an extension, both in the order of non-linearities and in the levels of coupling, of the model introduced by Paulling and Rosenberg (1959) and Paulling (1961). The equations are taken here in the explicit form described in detail in Neves and Rodríguez (2005, 2006). Thus, the non-linear heave, roll and pitch equations are introduced as:

$$\begin{aligned}&(m+Z_{\ddot z})\ddot z+Z_{\dot z}\dot z+Z_{\ddot\theta}\ddot\theta+Z_{\dot\theta}\dot\theta+Z_z z+Z_\theta\theta+\\&\frac{1}{2}Z_{zz}z^2+\frac{1}{2}Z_{\phi\phi}\phi^2+\frac{1}{2}Z_{\theta\theta}\theta^2+Z_{z\theta}z\theta+\frac{1}{6}Z_{zzz}z^3+\\&\frac{1}{2}Z_{zz\theta}z^2\theta+\frac{1}{2}Z_{\phi\phi z}\phi^2 z+\frac{1}{2}Z_{\phi\phi\theta}\phi^2\theta+\frac{1}{2}Z_{\theta\theta z}\theta^2 z+\\&\frac{1}{6}Z_{\theta\theta\theta}\theta^3+Z_{\zeta z}(t)z+Z_{\zeta\theta}(t)\theta+Z_{\zeta\zeta z}(t)z+Z_{\zeta zz}(t)z^2+\\&Z_{\zeta z\theta}(t)z\theta+Z_{\phi\phi\zeta}(t)\phi^2+Z_{\theta\theta\zeta}(t)\theta^2=Z_w(t)\end{aligned}\tag{1}$$

$$\begin{aligned}&(J_{xx}+K_{\ddot\phi})\ddot\phi+K_{\dot\phi}\dot\phi+K_{\dot\phi|\dot\phi|}\dot\phi|\dot\phi|+K_\phi\phi+K_{z\phi}z\phi+\\&K_{\phi\theta}\phi\theta+\frac{1}{2}K_{zz\phi}z^2\phi+\frac{1}{6}K_{\phi\phi\phi}\phi^3+\frac{1}{2}K_{\theta\theta\phi}\theta^2\phi+\\&K_{z\phi\theta}z\phi\theta+K_{\zeta\phi}(t)\phi+K_{\zeta\zeta\phi}(t)\phi+K_{\zeta z\phi}(t)z\phi+\\&K_{\zeta\phi\theta}(t)\phi\theta\ =0\end{aligned}\tag{2}$$

$$\begin{aligned}&(J_{yy}+M_{\ddot\theta})\ddot\theta+M_{\dot\theta}\dot\theta+M_{\ddot z}\ddot z+M_{\dot z}\dot z+\\&M_z z+M_\theta\theta+\frac{1}{2}M_{zz}z^2+\frac{1}{2}M_{\phi\phi}\phi^2+\frac{1}{2}M_{\theta\theta}\theta^2+\\&M_{z\theta}z\theta+\frac{1}{6}M_{zzz}z^3+\frac{1}{2}M_{zz\theta}z^2\theta+\frac{1}{2}M_{\phi\phi z}\phi^2 z+\\&\frac{1}{2}M_{\phi\phi\theta}\phi^2\theta+\frac{1}{2}M_{\theta\theta z}\theta^2 z+\frac{1}{6}M_{\theta\theta\theta}\theta^3+M_{\zeta z}(t)z+\\&M_{\zeta\theta}(t)\theta+M_{\zeta\zeta z}(t)z+M_{\zeta zz}(t)z^2+M_{\zeta\zeta\theta}(t)\theta+\\&M_{\zeta z\theta}(t)z\theta+M_{\phi\phi\zeta}(t)\phi^2+M_{\theta\theta\zeta}(t)\theta^2=M_w(t)\end{aligned}\tag{3}$$

On the left hand side of Eqs. (1-3), added masses and wave damping terms are assumed linear. A quadratic roll damping is considered in equation (2). The terms associated with variables z,ϕ,θ and wave elevation $\zeta(t)$ correspond to the non-zero linear and non-linear (up to third order) coefficients due to hydrostatic and wave pressure effects analytically derived by Neves and Rodríguez (2005, 2006), dependent on hull characteristics and on wave amplitude, frequency and time. On the right hand side of Eqs. (1-3), $[Z_W(t)\quad K_W(t)\quad M_W(t)]^T$ represent linear wave excitation. Due to the particular wave incidence considered, $K_W=0$ has been assumed in Eq. (2). Once all the coefficients in Eqs. (1-3) are known, this set of three equations may be numerically integrated without difficulty.

3. NUMERICAL LIMITS OF STABILITY

Numerical simulations have been performed in the case of a fishing vessel denominated TS. Details of the ship are given in Fig. 1 and Table 1. Parametric rolling of this fishing vessel has been experimentally and numerically examined in detail in Neves and Rodríguez (2005, 2006), Neves et al. (2002). Numerical simulations performed using equations (1-3) have been successfully compared to experimental results for different wave conditions and ship speeds. It was verified that the fishing vessel employed in the present investigation is quite prone to strong parametric rolling in head seas.

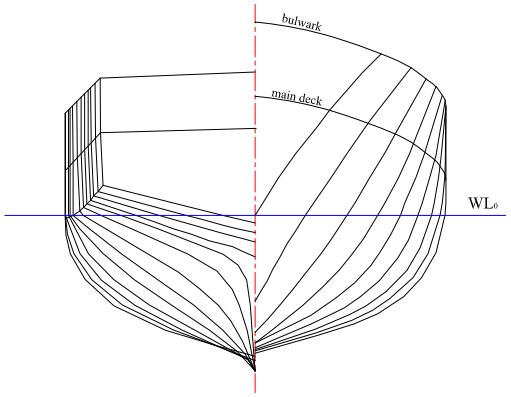

Figure 1. Hull form of transom stern (TS) fishing vessel.

Table 1. Ship main characteristics.

Denomination		**Ship TS**
Overall length	[m]	25.91
Length between perpendiculars	[m]	22.09
Breadth	[m]	6.86
Depth	[m]	3.35
Draft	[m]	2.48
Displacement	[ton]	170.3
Longitudinal radius of gyration	[m]	5.52
Metacentric height	[m]	0.37

Table 2. Two sets of initial conditions.

	I.C.#01	***I.C.#02***
z_0 (m)	0.00	0.00
$\dot{z}_0$ $(m/\sec)$	0.01	0.01
ϕ_0 (deg)	2.00	2.50
$\dot{\phi}_0$ (deg/sec)	-0.50	-0.80
θ_0 (deg)	0.00	0.00
$\dot{\theta}_0$ (deg/sec)	0.01	0.01

It is important to investigate parametric rolling not only at the *exact* encounter frequency tuning $w_e / w_{n4} = 2.0$. In fact, large amplifications may take place in a quite broad spectrum of excitations frequencies. In order to comprehensively investigate the unstable regions Neves and Rodríguez (2007b) proposed the computation of numerical maps representing the boundaries of stability but containing information on the amplitude of roll response in the whole region of parametric amplification. Figure 3 shows the limits of stability of the fishing vessel in head seas at Fn = 0.30, corresponding to the first region of instability. The mapping is constructed by numerically computing the roll amplitude for different encounter frequencies and wave amplitudes. All points of the map are computed for the set of initial conditions I.C.#01 defined in Table 2. The intensity of the final roll amplitude is indicated by the color scale displayed on the right hand side of the figure.

Four important features of the new limits of stability are:

- the appearance of upper boundaries, indicating that for increased wave amplitudes, parametric rolling may not necessarily increase; in fact, it tends to disappear.
- a general tendency of the unstable area to bend to the right, indicating that the exact tuning $w_e / w_{n4} = 2.0$ is not necessarily the tuning with stronger amplifications.
- smooth growth of roll amplitude at lower level of boundaries, abysmal (sudden) decrease in the upper boundaries.
- upper boundaries with fractal geometry.
- larger area of instability as the roll initial conditions were modified.

The last three characteristics point out to complexities and intricacies that demand further investigations. A more detailed discussion of these features may be found in Neves and Rodríguez (2007a). In the next section some numerical tools of nonlinear dynamics will be employed in an attempt to clarify some of these topics.

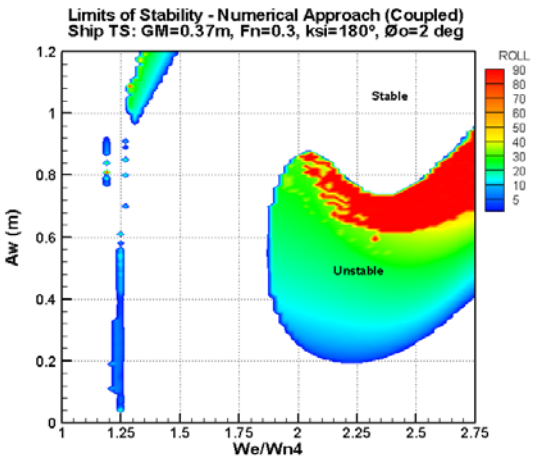

Figure 2. Limits of stability, ship TS, Fn=0.30, I.C.#01.

4. BIFURCATION DIAGRAMS

In Figure 2 the whole spectrum of exciting frequencies was explored. It has been observed that distinct characteristics are revealed. It is now desirable to get an in depth knowledge of dynamical characteristics as the parameter wave amplitude A_W is increased. So, if previously we have been more interested in the limits of stability as a whole, now we wish to have a closer look at some domains inside the unstable area. For this purpose, we will investigate the changes in dynamic characteristics as we cross the area inside the limits. A limited region of the map of limits of stability will be explored, that is, we will follow a vertical line defined at the tuning $w_e / w_{n4} = 2.0$ in Figure 2. Aiming at demonstrating the influence of initial conditions on the solutions corresponding to points inside the area of the limits of stability we developed a *brute-force* algorithm for capturing the branching of solutions for a specified set of initial conditions.

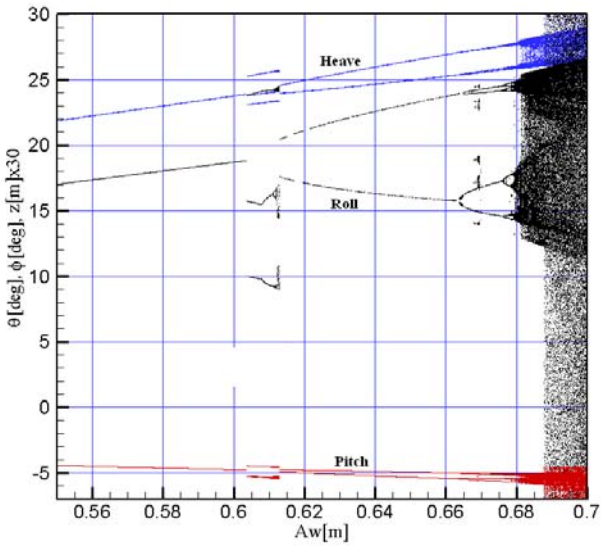

Figure 3. Heave, roll and pitch bifurcation diagrams, Fn=0.30, I.C.#01.

Thus, using the A_W parameter, the type of bifurcation diagrams as shown in Figure 3 for the heave, roll and pitch motions are developed for the same set of initial conditions used in the mapping of the limits of stability. These diagrams reveal the branching structure for distinct ranges of wave amplitude; qualitative and quantitative types of responses are noticed. These distinct results may be summarized as shown in Table 3.

Table 3. Roll solutions for Fn=0.30.

Range of Aw (m)	Type of roll response
0.0000 - 0.6036	Typically linear
0.6037 - 0.6129	period-3
0.6130 - 0.6626	Multistability, period-1
0.6627 - 0.6758	Multistability, period-2
0.6759 - 0.6782	Multistability, period-4
0.6783 - 0.67881	Multistability, period-8
0.67882 - 0.7000	Chaos

Two interesting characteristics, not observable in the numerical limits of stability, are revealed by this bifurcation analysis. First, in the short second range of A_W one observes the appearance of a solution with 3 periods that ends with a sudden appearance of a burst of non-periodic solutions. The period-3 solutions of heave, roll and pitch motions are illustrated in Figures 4-6, respectively. In each of them time history, phase plane and Poincaré map are shown. The appearance of non-periodic solutions is illustrated in Figure 7 which shows the roll time series, the corresponding phase diagram and Poincaré map for *Aw=0.6129 m.*

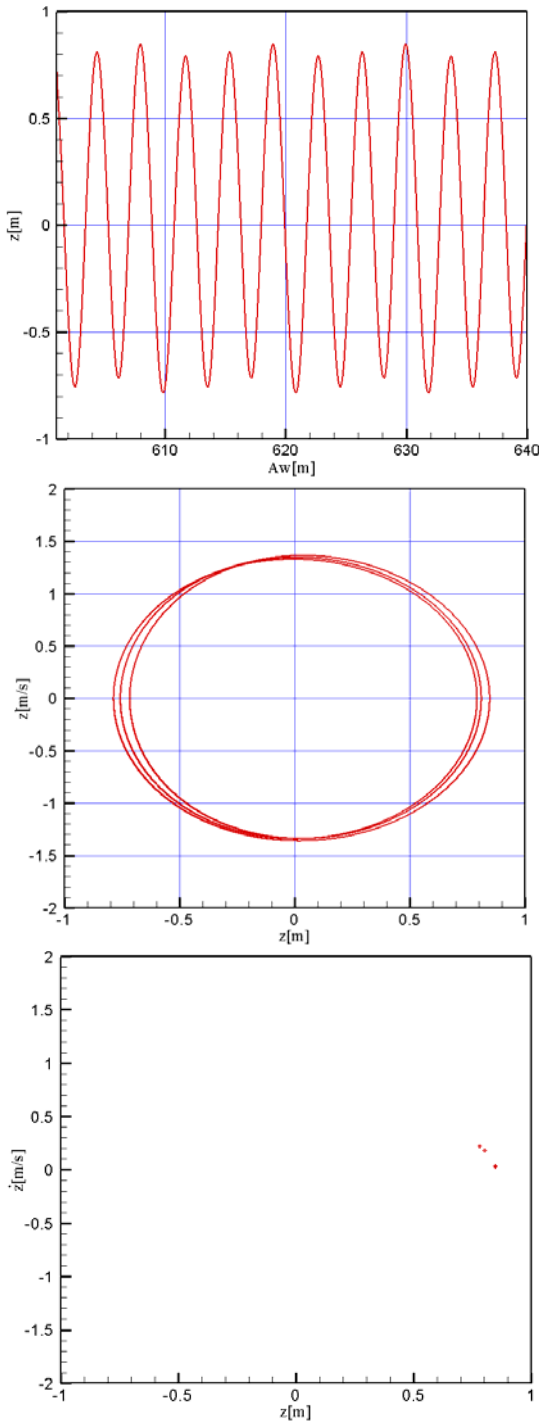

Figure 4. Heave motion, phase plane and Poincaré map, period-3 solution, Aw=0.605 m, I.C.#01.

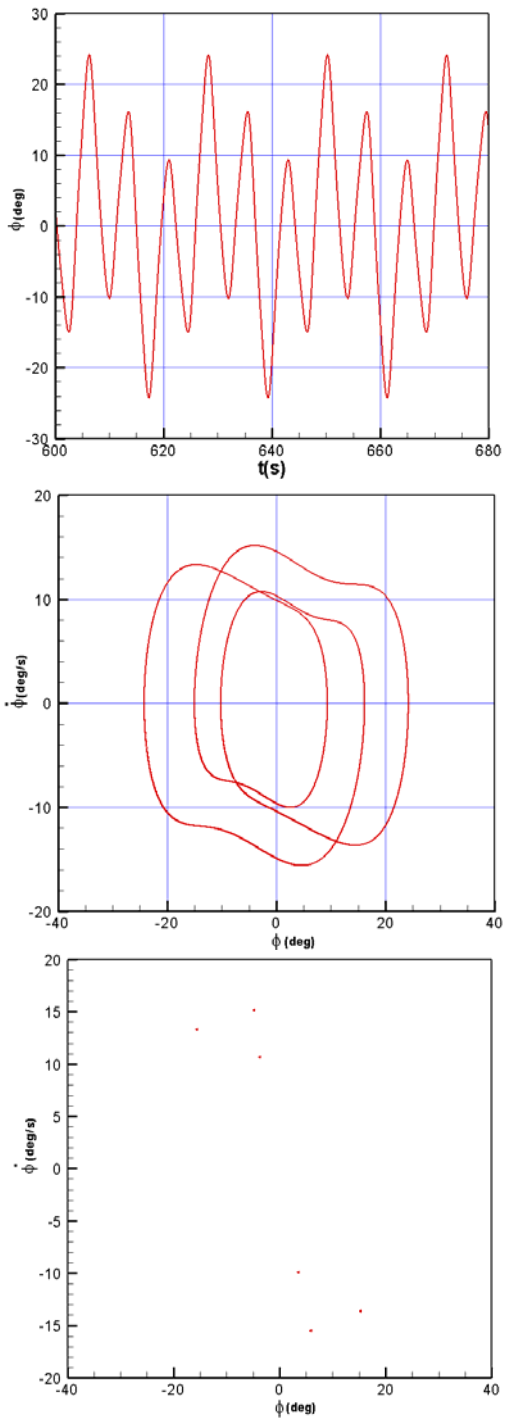

Figure 5. Roll (ϕ_{max}=24.18°), phase plane and Poincaré map, period-3 solution, Aw=0.61 m, I.C.#01.

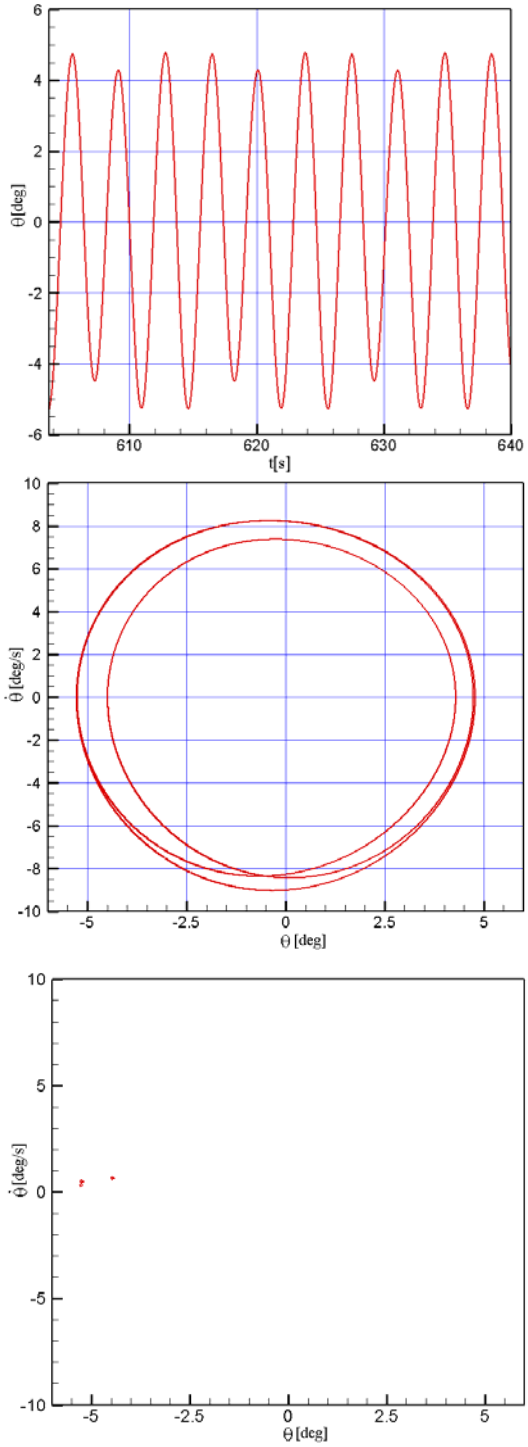

Figure 6. Pitch motion, phase plane and Poincaré map, period-3 solution, Aw=0.605 m, I.C.#01.

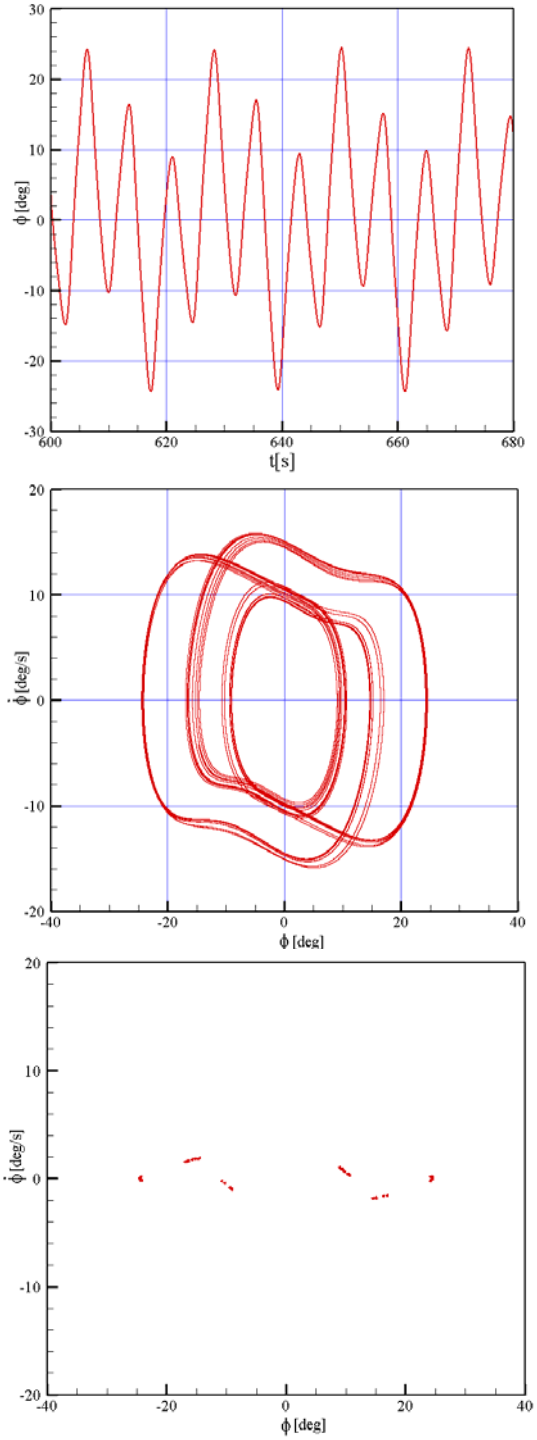

Figure 7. Roll motion, phase plane and Poincaré map, Aw=0.6129 m, I.C.#01. Non-periodic solutions.

The second interesting characteristic encountered is multistability with associated alternance of values. This dynamical feature arises immediately after the occurrence of a burst of non-periodic solutions, as shown in Figure 3. In the bifurcation diagram one may get the impression that the motion has migrated to a period-2 solution, but a detailed analysis will show that this is not the case. In fact the roll solutions in the third range of *Aw* are period-1, but as illustrated in Figures 8 and 9, the solutions continuously alternate from one attractor to another one which is situated close by, at each new value of the parameter *Aw*. In other words, roll motion either lives in one attractor or in the other, but always with a single period. Subsequently, for higher wave amplitudes, flip bifurcation will take place together with multistability: period-2, 4 and 8 solutions will appear in sequence ending in chaos.

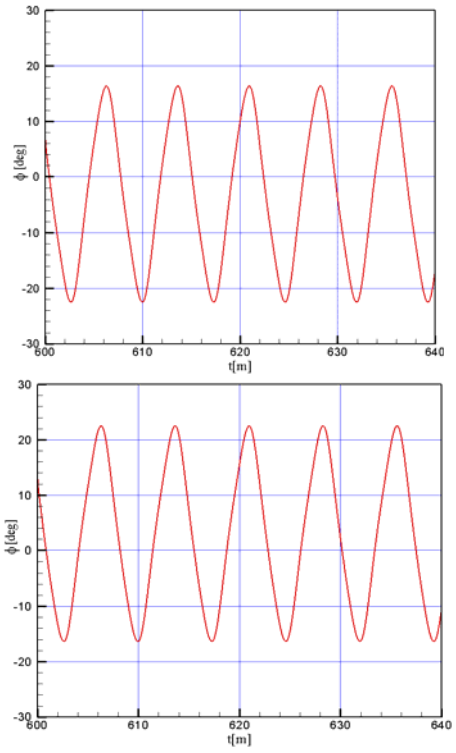

Figure 8. Roll motion: (a) Aw=0.639 m, (b) Aw=0.6391 m. Multistability for two neighboring points, I.C.#01.

It is interesting to observe that in this third range of Aw (0.6130 - 0.6626) the roll motion undergoes multistability with period-1 solutions, as shown in Figures 8 and 9. But in this same range, the vertical motions have already undergone a period doubling bifurcation. This is shown in Figures 10 and 11 for heave and pitch, respectively. Another aspect worth noting is that the alternating process does not contaminate these modes, Vivanco (2009).

Subsequently, in the fourth range of Aw (0.6627 - 0.6758) the roll motion continues with multistability but responding with period-2 solutions, as shown in Figure 12, whereas the heave and pitch motions now respond with period-4 solutions. The sequence of flip bifurcations soon leads the coupled system to respond with chaotic motions. Figure 13 illustrates the period-4 roll motion and finally, Figure 14 shows the chaotic behaviour for Aw=0.683 m. The region with chaotic behaviour ends abruptly at the wave amplitude corresponding to the upper limit of stability of Figure 2.

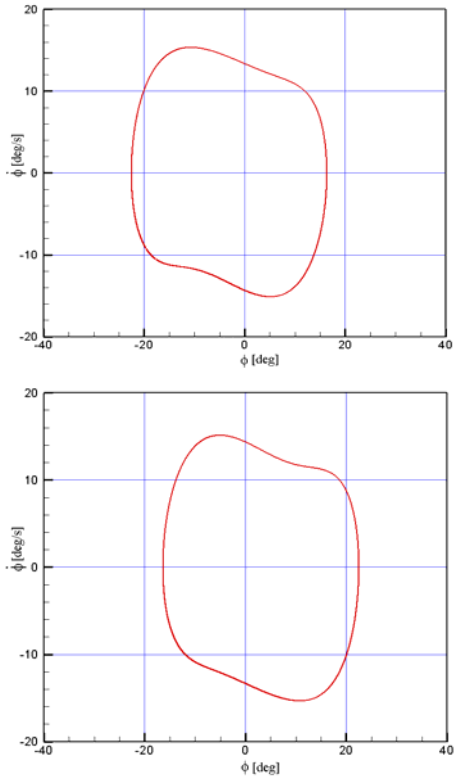

Figure 9. Roll phase planes: (a) Aw=0.639 m, (b) Aw=0.6391 m. Multistability for two neighboring points, I.C.#01.

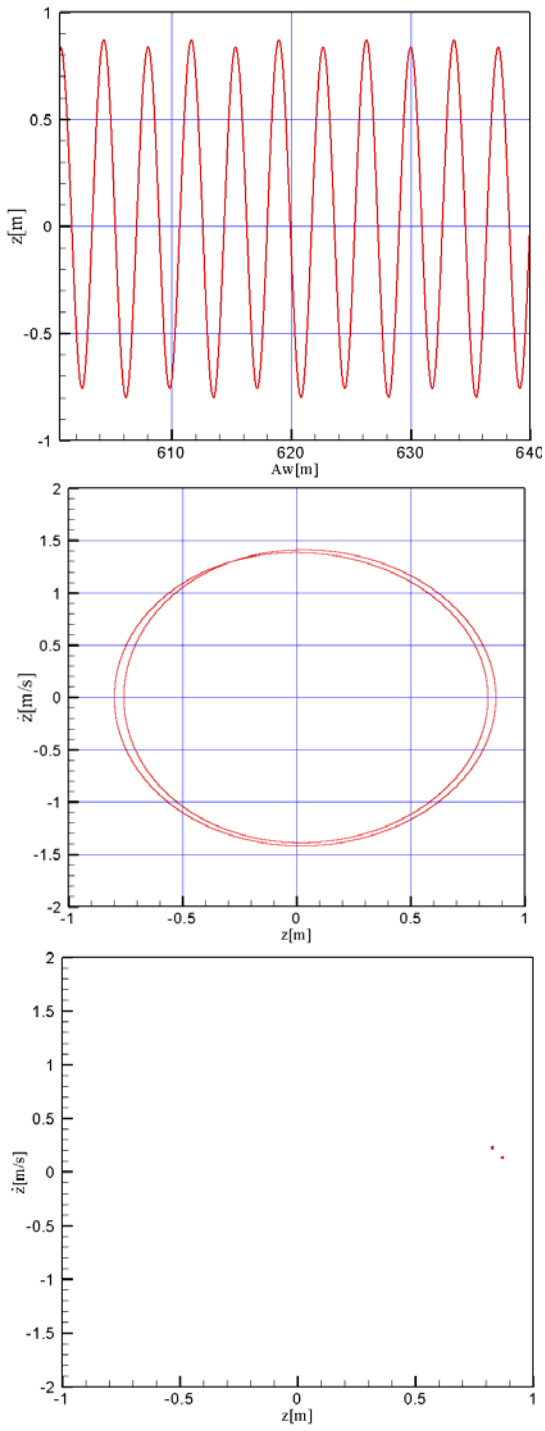

Figure 10. Heave time history, phase plane and Poincaré map, period-2 solution, Aw=0.64 m, I.C.#01.

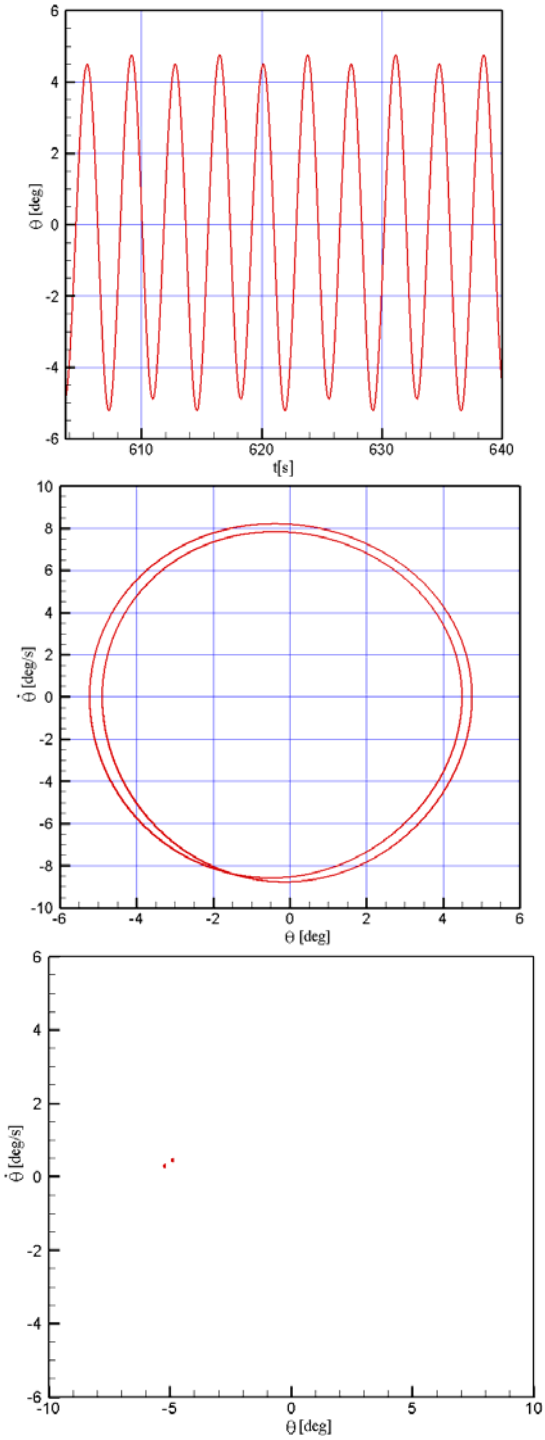

Figure 11. Pitch time history, phase plane and Poincaré map, period-2 solution, Aw=0.64 m, I.C.#01.

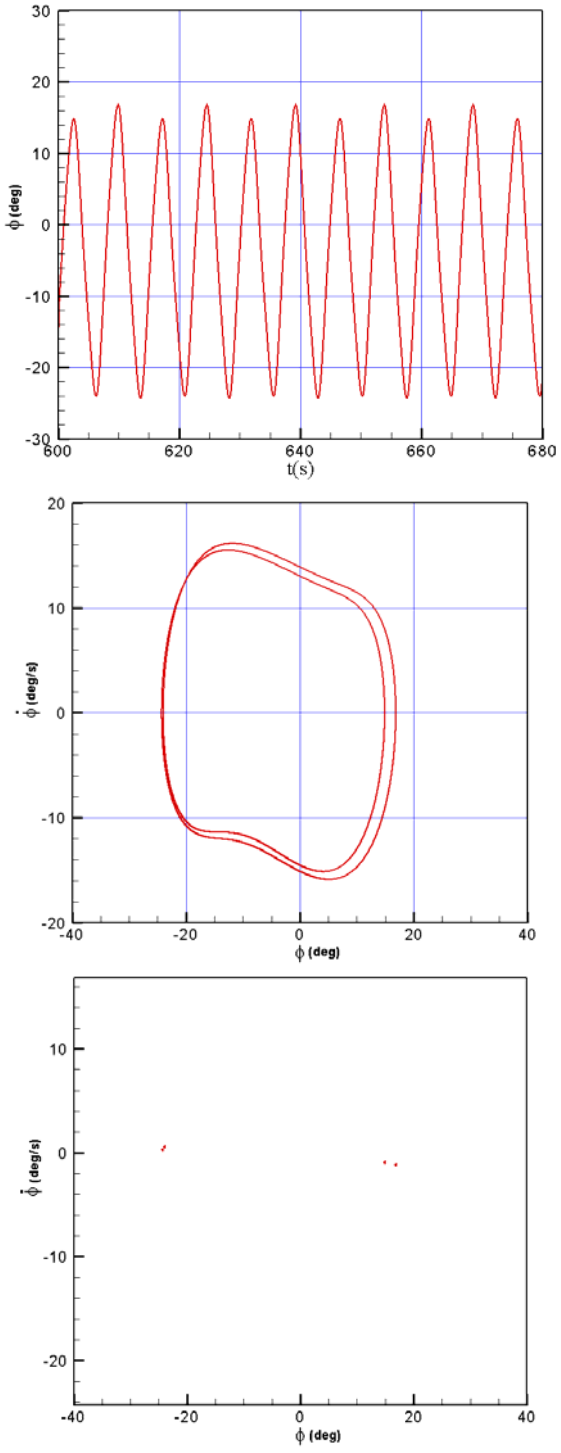

Figure 12. Roll motion (ϕ_{max}=24.27°), phase plane and Poincaré map, period-2 solution for Aw=0.67 m, I.C.#01.

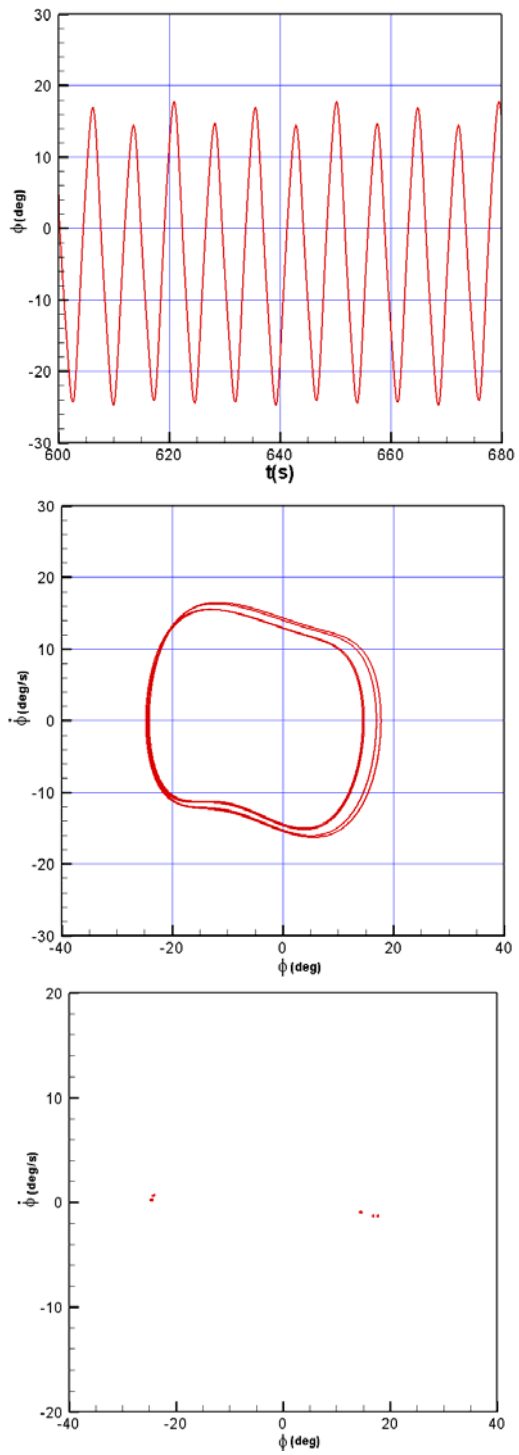

Figure 13. Roll motion (ϕ_{max}=24.73°), phase plane and Poincaré map, period-4 solution for Aw=0.678 m, I.C.#01.

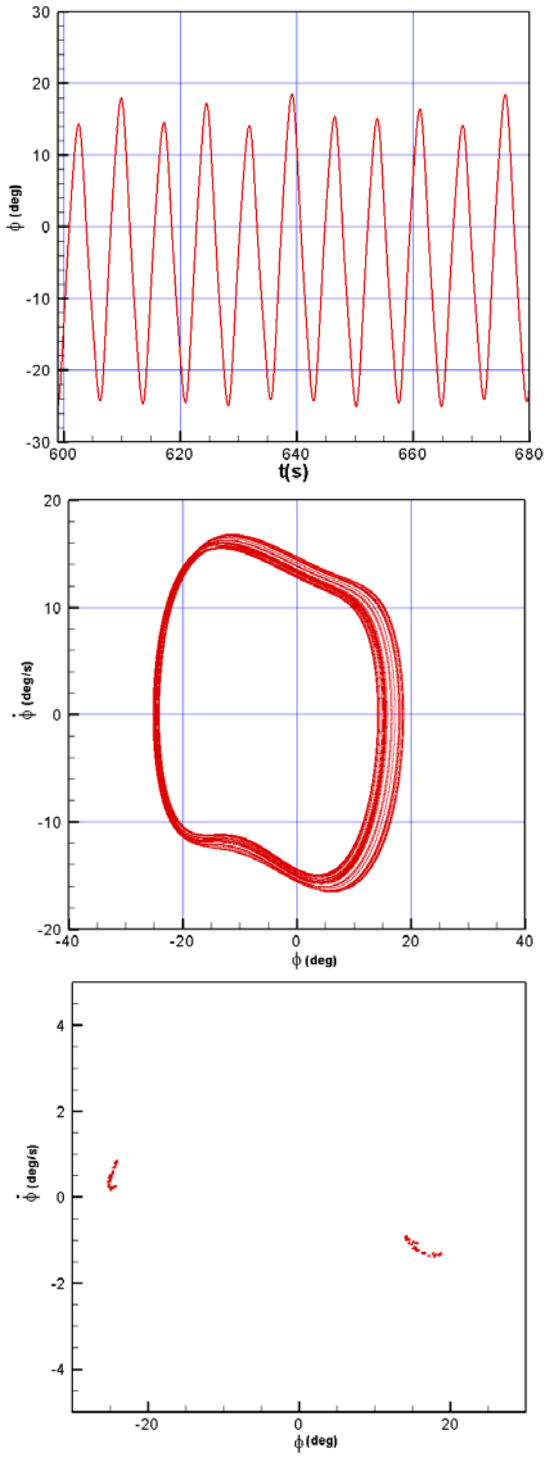

Figure 14. Roll motion (ϕ_{max}=25°), phase diagram and Poincaré map, chaotic behaviour for Aw=0.683 m, I.C.#01.

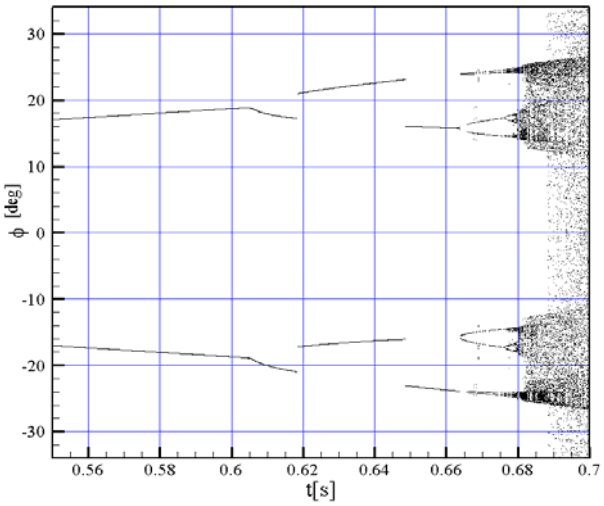

Figure 15. Roll bifurcation diagram, Fn=0.30, I.C.#02.

To illustrate the dependency of the limits of stability on initial conditions, a second set of initial conditions (I.C.#02) defined in Table 2 is considered. When initial conditions are changed, the general bifurcation set is preserved, but it may be observed in the new bifurcation diagram that, as shown in Figure 15, the range of responses with period-3 solution simply is not reached. At $A_W = 0.617m$ the motion jumps to a higher value. Instead of alternating continuously, the roll motion now undergoes period-1 motions with jumps, the first one producing a jump from 17 to 21 degrees. A second jump takes place at $A_W = 0.648m$, from 24 to 16 degrees. At $A_W = 0.663m$ the motion begins a flip bifurcation at the same point as obtained in Figure 3. Period-2, 4, 8 solutions appear in cascade, at all stages featuring multistability. Finally, chaotic motions take place again for $A_W \geq 0.6788m$.

5. LYAPUNOV EXPONENTS

Lyapunov exponents offer a quantitative measure of the sensitivity of a nonlinear dynamic system to initial conditions. As such, they characterize the chaotic behaviour of the system. The Lyapunov exponents provide information on the global stability of the system: values obtained for these exponents,

after the transients, are negative for stable zones, zero at bifurcation and positive in the chaotic zones. The method of trajectories developed by Wolf and Vastago (1985) is employed here in order to compute all the exponents relative to the heave, roll and pitch coupled motions for the tuning $w_e / w_{n4} = 2.0$ and different wave amplitudes. Figures 16 and 17 show the six exponents for two wave amplitudes, Aw=0.62 m and Aw=0.63 m, respectively. In Figure 16 all exponents are negative, with the larger one being quite close to zero, whereas in Figure 17 this larger exponents is practically zero. Compiling the values of the Lyapunov exponents obtained for varying wave amplitudes at *t=800 sec*, Figure 18 gives a complete picture of the evolution of the first three larger exponents, with the control parameter Aw, showing that at Aw=0.63 m the system undergoes chaos. This indicates that other attractors may be competing with those observed in Figures 3 and 15. In any case, this result demonstrates that the motions shown in Figure 7, corresponding to Aw=0.6129 m are non-periodic, not chaotic.

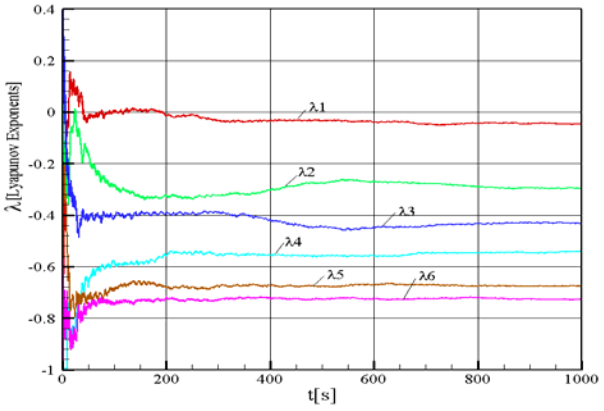

Figure 16. Lyapunov exponents, Aw=0.62 m.

6. CONCLUSIONS

Numerical limits of stability for a fishing vessel at Fn=0.30 undergoing strong parametric rolling in head seas have been computed for a range of encounter frequencies. The main dynamical characteristics of these limits have been discussed.

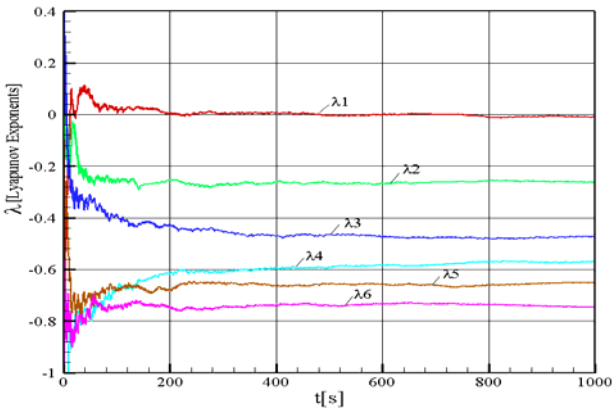

Figure 17. Lyapunov **e**xponents, Aw=0.63 m.

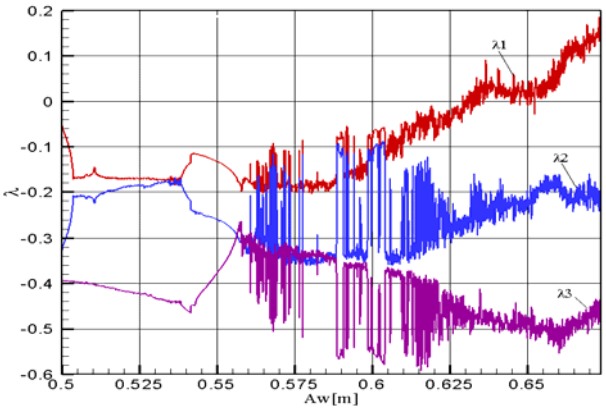

Figure 18. Lyapunov exponents (t=800 sec) for different wave amplitudes.

For the encounter frequency tuning corresponding to the first region of instability of the Mathieu stability map, bifurcation diagrams for the heave, roll and pitch motions have been computed considering wave amplitude as control parameter. Interesting phenomena such as coexistence of attractors with period-3 solutions, appearance of a burst of non-periodic solutions, multistability with alternance, fold and flip bifurcation and chaos have been identified. The phase planes and Poincaré mappings showed that the period-3 solutions and burst of non-periodic solutions are common to the three modes of motion considered. On the other hand, multistability with alternance only takes place for the roll motion. It was observed that when a different

set of initial conditions was considered, both the non-periodic motions and alternance disappeared. Finally, Lyapunov exponents have been computed for the same encounter frequency tuning, again taking the wave amplitude as control parameter.

7. ACKNOWLEDGEMENTS

The present investigation is supported by CNPq within the STAB project (Nonlinear Stability of Ships). The Authors also acknowledge financial support from CAPES, FAPERJ and LabOceano. Thanks are due to Prof. Marcelo A. Savi for many fruitful discussions.

8. REFERENCES

Guckenheimer, J., and Holmes, P., 1983, "Nonlinear Oscillations, Dynamical Systems and Bifurcations of Vector Fields", Applied Mathematical Sciences, vol. 42, Springer-Verlag.

Neves, M.A.S. and Rodríguez, C., 2005, "A Nonlinear Mathematical Model of Higher Order for Strong Parametric Resonance of the Roll Motion of Ships in Waves", Marine Systems & Ocean Technology – Journal of SOBENA, Vol. 1 No. 2, pp. 69-81.

Neves, M.A.S. and Rodríguez, C., 2006, "Unstable Ship Motions Resulting from Strong Nonlinear Coupling", Ocean Engineering, vol. 33, pp. 99-108.

Neves, M.A.S. and Rodríguez, C., 2007a, "Influence of Nonlinearities on the Limits of Stability of Ships Rolling in Head Seas", Ocean Engineering. v.34, p.1618 – 1630.

Neves, M.A.S. and Rodríguez, C., 2007b, "An Investigation on Roll Parametric Resonance in Regular Waves", International Shipbuilding Progress, Vol 54, pp. 207-225.

Neves, M.A.S., Pérez, N.A. and Lorca, O., 2002, "Experimental Analysis on Parametric Resonance for Two Fishing Vessels in Head Seas", 6th International Ship Stability Workshop, Webb Institute, New York, USA.

Paulling, J.R. and Rosenberg, R.M, 1959, "On Unstable Ship Motions Resulting from Nonlinear Coupling", Journal of Ship Research 3 (1), 36-46.

Paulling, J.R., 1961, "The Transverse Stability of a Ship in a Longitudinal Seaway", Journal of Ship Research, vol. 4, no. 4 (Mar.), pp. 37-49.

Seydel R., 1988, "From Equilibrium to Chaos: Practical Bifurcation and Stability Analysis", Elsevier Science Publishing Co., Inc., NY.

Vivanco, J.E.M., 2009, "Parametric Rolling of a Fishing Vessel - Nonlinear Dynamics", M.Sc. Dissertation, COPPE/UFRJ, Jan (in Portuguese).

Wolf, A. and Vastago, A., 1985, "Determining Lyapunov Exponents from a Time Series", Physical Review 16D, pp. 25-317.